Theor Chem Account (2008) 121:247–255
DOI 10.1007/s00214-008-0470-3

REGULAR ARTICLE

Metal induced molecular nano-extraction

Aned de Leon · Abraham F. Jalbout

Received: 28 May 2008 / Accepted: 17 July 2008 / Published online: 18 September 2008

Abstract We have previously devised a "scorpion" like system which is composed of a zigzag (8,0) single walled carbon nanotube attached to a 20 ringed graphene sheet by a glycine dimer species. Theoretical density functional theory calculations on a potential mechanism driven by a metal induced charge transfer process has been proposed for the extraction of molecules from nanotubes.

Keywords Polar molecules · Metals · SWNT · Carbon sheet · DFT-BLYP

1 Introduction

The study of single walled nanotubes (SWNT) [1,2] has many important implications in the field of material science as well as catalysis [3–5]. The unique structural features of these materials permit for interesting elucidations and reactive mechanisms to be undertaken. Additionally, the mechanical and chemical stability of SWNT materials allows for functionalizations [6,7] to be performed. Multiple investigations suggest contribute to their ability to distribute peptides, DNA fragments in vivo.

The nanosystems under consideration present certain disadvantages that should be addressed. Their hydrophilicity leads to toxicity in biological systems which limit applications in drug design and discovery. Typically, carbon based systems are functionalized in order to resolve this problem and enhance polar molecular and aqueous interactions. These processes are local transformations that do not lead to problematic structural situations without modification of their physical properties.

The lack of specificity associated with SWNT materials is another issue of difficulty in performing chemical modifications on their surfaces. This is intrinsically related to the nature of the carbon atoms in the nanotubes which are similar. To alleviate this matter novel complexes have synthesized to promote chemical differentiation.

Theoretical calculations performed by our group suggest that nanotube systems can localize charge on their exterior as a result of charge transfer systems with endohedral metals. The effect that is related to this issue is correlated to studies of ion transfer mechanisms on molecular surfaces. Small polar molecules have been demonstrated to interact on the interior cavity of SWNT systems [8] and on the exterior [9]. Amino acids can favorably interact with biomolecules [10–12] as well as with nanostructures [13] to form peptide interconnected species. The tips of the SWNT molecules can be modified with organic groups [13] to form interesting frameworks that posses variable properties [14–18].

In the present work we have exploited the ability of polar molecules to be stabilized on the surface of graphene sheets to develop a molecular extraction nano-device. Recently, we localized polar species on localized regions of extended linear sheets [19] as well as to the interior of SWNT molecules [8]. While gold surfaces usually mediate connections of amino acids to SWNT structures [20] as a consequence of computational difficulties such models cannot be used.

To compensate we designed a "scorpion" shaped (based on its interesting structural features) that is composed of a zigzag (8,0) SWNT connected to a 20 ring carbon sheet [21].

A. de Leon · A. F. Jalbout
Instituto de Ciencias Nucleares, Universidad Nacional Autónoma de México, Circuito Exterior, Ciudad Universitaria, 04510 Mexico D.F., Mexico

A. F. Jalbout (✉)
Departamento de Investigacion en Fisica, Universidad de Sonora Hermosillo, Sonora, Mexico
e-mail: ajalbout@u.arizona.edu

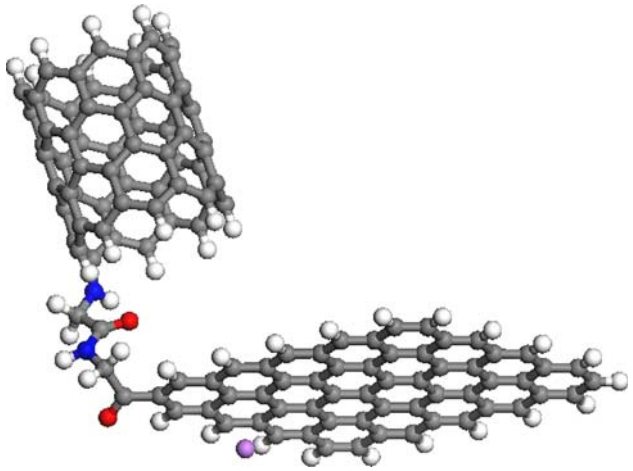

Scheme 1 Graphical representation of the Li[SWNT-Sheet] "scorpion" like system composed of a zigzag (8,0) system anchored to a two glycine (Gly) amino acid interconnect to a 20 ring graphene system. In the figure white spheres are hydrogen atoms, *blue spheres* are nitrogen atoms, *red spheres* are oxygen atoms, *grey spheres* are carbon atoms and finally the *purple sphere* is the lithium atom

We depicted that this "scorpion" structure can adequately encapsulate small polar molecules (HF, H_2O, H_2S, NH_3) into nanotubes using carbon sheets. Other work shows that charge transfer mechanisms from endohedral metals can influence the surface properties of nanosystems [22] and enhance molecular interactions [23]. In the study herein we will use metal localization on the carbon sheet to extract molecules from the interior of the nanotubes (see Scheme 1). Such a phenomena is due to the formation of "image potentials" that are capable of forming interactions underneath the surface of the carbon sheets to external partial polarizable molecules [24,25].

2 Computational methods

Density functional theory (DFT) calculations were performed with the DMol^3 [26] numerical-based density-functional computer software implemented in the Materials Studio Modeling 3.1 package from Accelrys, Inc. Geometry optimizations as well as frequency analysis calculations were done with the BLYP general gradient potential approximation (GGA) with the double-numerical plus diffusion basis set (all-electron core treatment) denoted as DND. The algorithms were carried out with standard convergence criteria and global orbital cutoffs were employed on basis set definitions. The expulsion energy has been defined as:

$$E^{\exp} = E_{\mathrm{Li[SWNT-Sheet]-MOL}} - (E_{\mathrm{Li[SWNT-Sheet]}} + E_{\mathrm{MOL}}), \quad (1)$$

whereby $E_{\mathrm{Li[SWNT-Sheet]-MOL}}$ is the energy of the complex with the polar molecule, $E_{\mathrm{Li[SWNT-Sheet]}}$ is the energy of the isolated Li[SWNT-Sheet] species and E_{MOL} is the energy of the small polar molecule. Additionally, the metal (in this case Li) adsorption to the carbon sheet has been defined as:

$$E^{\mathrm{ads}} = E_{\mathrm{[SWNT-Sheet]-MOL}} + E_{\mathrm{Li}} - E_{\mathrm{Li[SWNT-Sheet]}}. \quad (2)$$

The relative energy (ΔE) of the configurations is defined as:

$$\Delta E = E^{\mathrm{Sheet}}_{\mathrm{Li[SWNT-Sheet]-MOL}} - E^{\mathrm{Inside,Between}}_{\mathrm{Li[SWNT-Sheet]-MOL}}. \quad (3)$$

The latter term in Eq. (3) is the energy of the Li[SWNT-Sheet] complex with the polar molecule on the inside of the SWNT or between the SWNT and the sheet. The expulsion energy in Eq. (1) assists to quantify the energy needed to remove the polar molecule from the system. The adsorption energy denotes the affinity of the metal atom to the surface, and the final equation is the relative energy of various arrangements.

Throughout the structural designations, a zigzag (8,0) SWNT structure (that has a diameter of 6.3 Å and a length of 9.24 Å) that is connected a carbon sheet which is composed of 20 benzene rings (measuring a length of 18.7 Å with a width of 12.9 Å) by a peptide chain of two glycine molecules. Glycine is the simplest amino acid and larger peptide chains are computationally expensive. The attachment of the polar molecules and metal atoms was considered in many configurations to perform an adequate potential energy landscape search. From previous studies [8,9,21] we reported that the methods used reduce basis set superposition (BSSE) errors. The results obtained with other DFT routines (i.e. PW91, PBE, HCTH, BOP) and local density approximation (LDA) methods (i.e. VWN, PWC) were performed to ensure computational consistency. The BLYP functional employed partially accounts for dispersion and for experimental results available provides accurate and physically reasonable data.

3 Results and discussion

Scheme 1 is a graphical depiction of the engineered system by which the HF, H_2O, H_2S and NH_3 polar molecules were used to explore the interactions with the Li[SWNT-Sheet] system. The molecules that were implemented previously were used to adhere to the surface of the SWNT [9,21] and were used in the work herein. Table 1 shows selected thermochemical properties of the species in kcal/mol where $E^{\exp}$ is the expulsion energy of the polar species, E^{ads} is the adsorption energy of the binding of the polar molecule to the SWNT-Sheet system, ΔE are energy relative differences between the configurations and GAP is the HOMO/LUMO gap of the computed systems (the gap of the isolated system is 0.88 kcal/mol).

In the second table we display low-range frequencies for the species shown in Scheme 2 (in units of cm^{-1}). Figure 1 (for the HF and H_2O systems) and 2 (for the H_2S and NH_3

Table 1 Physical properties (in kcal/mol) of the clusters investigated whereby E^{exp} is the polar molecule expulsion energy, E^{ads} is the adsorption energy (of the Li atom), ΔE is the relative differences in energy between the configurations and GAP is the HOMO/LUMO gap of the compounds (the gap of the isolated system is 0.88 kcal/mol)

Property	HF	H_2O	H_2S	NH_3
Inside				
E^{exp}	5.13	0.56	7.08	1.31
E^{ads}	−234.84	−230.71	−950.54	−231.89
ΔE	10.91 (8.94)	16.79 (9.99)	32.54 (19.25)	22.74 (7.97)
GAP	1.51	1.59	1.79	1.52
Between				
E^{exp}	16.05	17.36	17.45	23.77
E^{ads}	−236.82	−238.00	−963.83	−246.65
ΔE	0.00 (4.34)	0.00 (1.84)	0.00 (0.376)	0.27 (2.13)
GAP	1.16	1.94	1.71	1.55
Sheet				
E^{exp}	14.16	15.61	13.98	24.05
E^{ads}	−239.27	−237.58	−962.72	−248.78
ΔE	1.89 (0.00)	1.75 (0.00)	1.48 (0.00)	0.00 (0.00)
GAP	2.00	1.83	1.59	1.64

The values in parenthesis correspond to the non-metal [SWNT-Sheet] affinities from Ref [21]

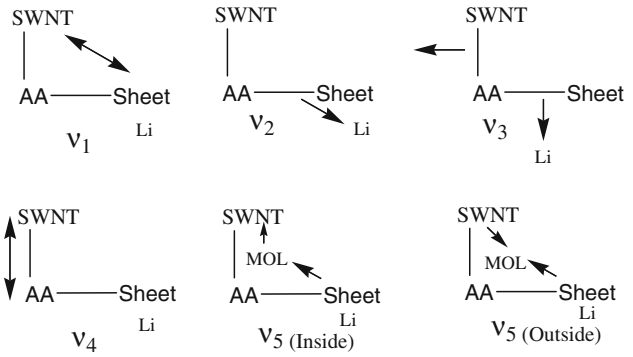

Scheme 2 Vibrational mode characterization for the frequencies denoted in Table 2, whereby SWNT is the zigzag (8,0) system, Sheet is the carbon sheet, AA is the glycine dimer, Mol is the small polar species. Also, ν_5 (*inside*) is the coupling of the small polar molecule to the interior wall of the SWNT and ν_5 (*outside*) is the coupling of the polar molecule to the SWNT and the carbon sheet

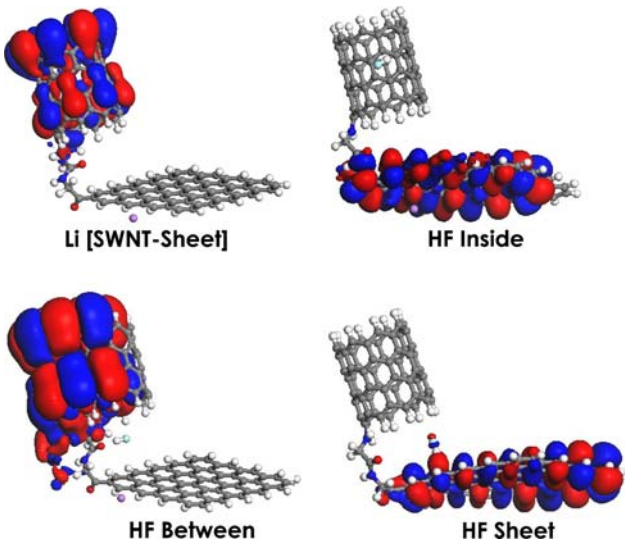

Fig. 1 HOMO plots (at a 0.02 a.u. contour level) for the HF system displayed where the same coloring scheme as in 1 is applied (except for fluorine which is depicted in *green*)

systems) denotes various geometrical parameters where bond lengths are in angstroms (Å) and bond angles are in degrees (°). It is important to mention that the $\nu_1 - \nu_5$ modes correspond to the Li[SWNT-Sheet] stretching modes, the Sheet rocking mode, the Li[SWNT-Sheet] rocking mode, the amino acid chain (which is composed of two molecules of Glycine)-SWNT stretching mode, and SWNT-MOL-Sheet-Li coupling modes (whereby MOL is the polar molecule under consideration), respectively. Figure 3 shows a HOMO electronic density plot of the Li[SWNT-Sheet]-HF systems as an example case.

3.1 HF-[SWNT-Sheet] system

We will first consider the interaction of hydrogen fluoride (HF) with the Li[SWNT-Sheet] system (HOMO plot in Fig. 1, geometrical parameters in 2). From the figure we can see that in the first species (whereby HF is on the sheet) the distance is around 3.4 Å. Many configurations have been searched for by modification of the positions of the polar molecules as well as the metals. Additionally, the conformational rotations along the axis of the amino acid chain was attempted to ensure

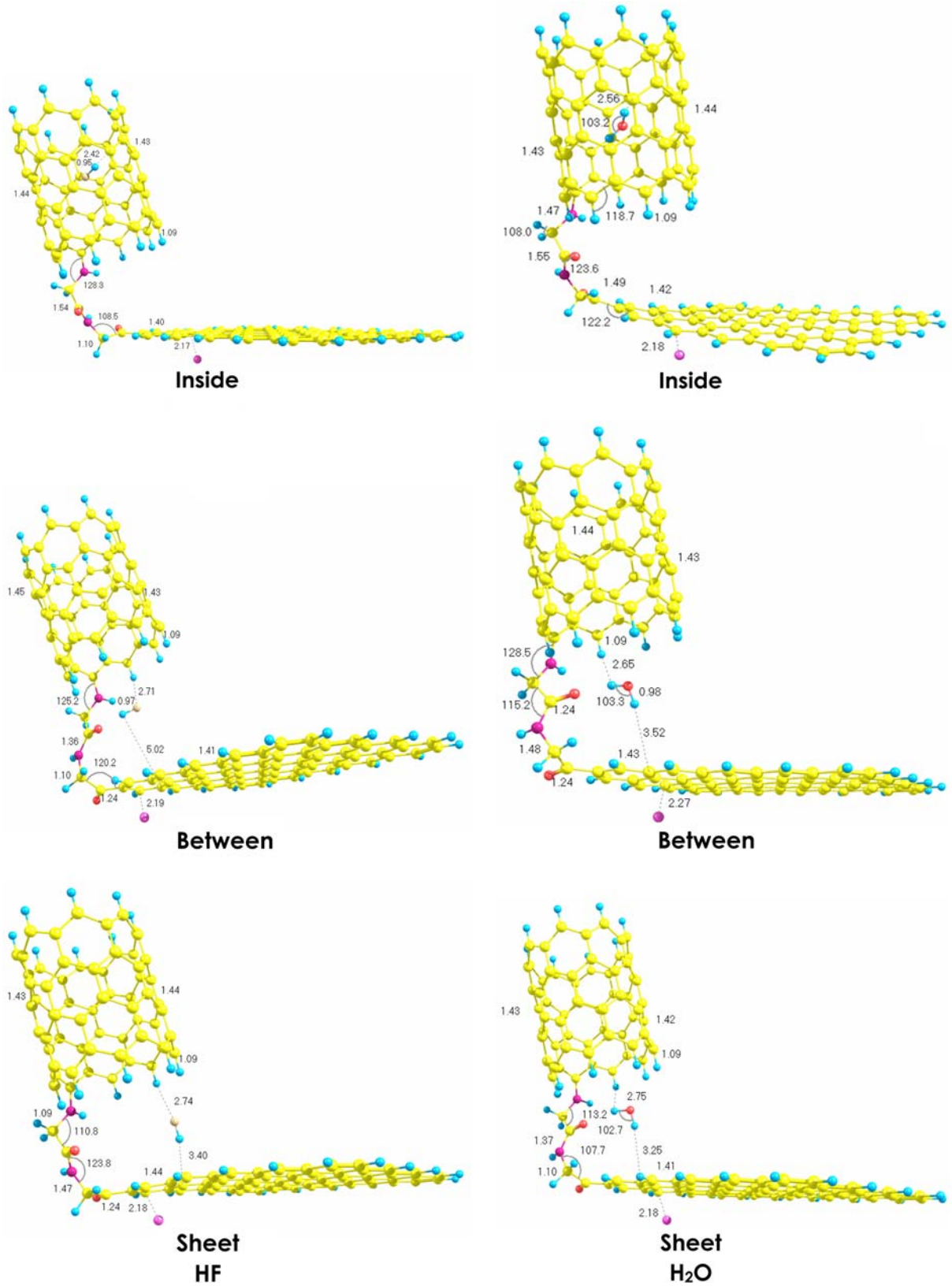

Fig. 2 Geometrical parameters of the HF and H_2O systems whereby bond lengths are in angstroms (Å) and bond angles are in degrees (°). The coloring scheme is as follows: *blue spheres* are hydrogen atoms, *dark purple spheres* are nitrogen atoms, *red spheres* are oxygen atoms, *yellow spheres* are carbon atoms, the *orange sphere* is fluorine, and finally the *purple sphere* is the lithium atom

that the structures obtained were the lowest energy structures feasible.

Table 1 displays the energy of adsorption of the metal species in the "sheet" configuration is around −239.3 kcal/mol and the energy of expulsion is 14.16 kcal/mol. While the configuration with the polar molecule in between the SWNT and the sheet is stabilized the barriers are reduced upon metal adsorption (the values in parenthesis correspond to the non-metal cases). The HOMO/LUMO gap rises in the polar molecule configurations in comparison to the isolated cases, but it is not large. The vibrational frequencies are similar in the cases studied whereby the largest deviation is for the Li[SWNT-Sheet] rocking mode (ν_3) that is attributed to the placement of the metal atom.

The next species studied is the lowest energy structure whereby the HF molecule is localized at a distance of 5.02 Å to the sheet and 2.71 Å to the SWNT. The adsorption energy is −236.8 kcal/mol with expulsion energy of 16.05 kcal/mol and a HOMO/LUMO gap of 1.16 kcal/mol that is lower than the previous case. This can lead to the stability of this complex as a result of its ability to mediate the charge donated by the Li atom between the SWNT and the carbon sheet. The difference in energy between the "sheet" and "between" configuration is the transition energy for the movement of the polar molecule along the graphene surface.

The final structure in which the HF molecule is localized in the interior of the SWNT molecule at a distance of 2.42 Å from the wall of the surface has a ΔE of 10.91 kcal/mol. The expulsion energy is about 5.13 kcal/mol and an adsorption energy of −234.8 kcal/mol with a HOMO/LUMO gap of 1.51 kcal/mol. Upon metal encapsulation the barrier for SWNT expulsion increases making it easier to remove the molecule from the interior cavity.

The SWNT-MOL-Sheet-Li coupling mode (ν_4) increases in the sheet complex as can be seen from Table 2. This can be attributed to the intermolecular separation and the orbital coupling of the HF molecule to the molecular sheet. The other vibrational modes are rather consistent among the species studied. What is interesting to note is that the metals permits the surface to localize the polar molecule and improve its affinity.

Figure 1 shows the HOMO electronic density plot (at a contour level of 0.022 a.u.) for the Li[SWNT-Sheet] case as well as Li[SWNT-Sheet]-HF case. This has been used to represent the bonding character in the remainder of the structures under consideration for the interest of space. As we can see in the isolated Li[SWNT-Sheet] case the electron density is localized on the SWNT system, and when the HF is located on the interior of the framework the electron density is located on the surface of the sheet. When the HF species are in the "between" configuration the electron density is localized again on the SWNT molecule that can better mediate the charge as a result of the highly aromatic nature of this moiety. The polar molecule in essence attempts to act as a charge buffer between the charge induced on the graphene surface and the SWNT. In the final case, when the HF species is localized on the sheet the molecule solvates the excess electron density on the surface of the sheet as can be seen. This result increases the total energy of this configuration in comparison to the between configuration based on electron density distribution contributions.

Table 2 Low-range vibrational modes (denoted in 2) for the molecules studied in cm^{-1}

Property	ν_1	ν_2	ν_3	ν_4	ν_5
SWNT-sheet	34.6	111.5	211.0	339.5	–
Li [SWNT-sheet]	29.9	107.7	213.6	339.0	–
HF					
Inside	37.2	111.3	227.4	340.9	430.0
Between	33.8	110.5	220.5	338.9	424.6
Sheet	35.2	104.2	223.2	340.1	422.5
H_2O					
Inside	38.4	105.0	228.6	340.0	433.5
Between	35.2	104.2	233.5	340.1	436.9
Sheet	32.0	109.9	235.7	346.2	435.7
H_2S					
Inside	38.0	109.6	236.4	342.4	442.7
Between	38.3	108.4	231.4	338.1	443.6
Sheet	39.7	107.1	238.3	339.9	444.3
NH_3					
Inside	29.3	129.4	237.7	344.1	437.1
Between	84.5	125.5	237.2	341.6	434.0
Sheet	32.2	124.8	239.2	340.8	436.8

3.2 H_2O-[SWNT-Sheet] system

The next system under consideration is the interaction of water (H_2O) with the Li[SWNT-Sheet system] (displayed in 2). In the first species we can see that when the water is localized on the sheet the distance to the surface is around 3.25 Å with a HOMO/LUMO gap of around 1.83 kcal/mol. The higher end vibrational mode frequencies ($\nu_3 - \nu_4$) are larger for this system than those with the polar molecule present. The transition energy from the "between" configuration to this complex is around 1.75 kcal/mol which is still within reason.

The movement of the water molecule to a conformation that is between the SWNT and sheet structure is the lowest energy structure in this example. This complex occurs at a distance of around 3.52 Å from the sheet and 2.65 Å from the SWNT surface. The associated HOMO/LUMO gap of this complex is 1.94 kcal/mol with an expulsion energy of 17.36 kcal/mol and a relatively large adsorption energy of −238.0 kcal/mol. The final movement is the energy barrier

associated with encapsulating the polar molecule which has a barrier of around 16.79 kcal/mol which is significantly larger than the non-metal case. The strongest vibrational coupling is the Li[SWNT-Sheet] stretching modes (ν_1) with a minimal expulsion energy of 0.56 kcal/mol. The HOMO/LUMO gap of this complex is smaller than the previous cases but the polar molecule still prefers to occupy a site in between the SWNT and the carbon sheet system to mediate the charge density from the metal atom.

3.3 H_2S-[SWNT-Sheet] system

In this system we will study the effect of the interaction of hydrogen sulfide (H_2S) with the Li[SWNT-Sheet system] (depicted in Fig. 3). The first system when it is localized on the sheet has an intermolecular separation of 2.79 Å with the sheet with a HOMO/LUMO gap of 1.59 kcal/mol and a relative energy of 1.48 kcal/mol. The adsorption energy is quite high, suggesting a unique interaction between the excess electron the H_2S molecule which is a phenomena that we have previously asserted [26]. The theoretical vibrational modes for ν_3 are significantly elevated as a result of the coupling to the polar molecule.

Movement of the polar species to a configuration that is between the SWNT and the sheet at distances of 3.01 and 3.24 Å, respectively, leads to the most stable configuration. This species has an expulsion energy of 15.45 kcal/mol with a HOMO/LUMO gap of 1.71 kcal/mol. The final structure leads to a configuration by which the polar molecule is located a distance of 2.63 Å from the walls of the SWNT. The associated barrier is 32.54 kcal/mol with an expulsion energy that is lower than the previous cases considered. The barriers associated to move from the sheet and between the SWNT and sheet is minimal, but the barriers to move into the SWNT are larger than previously calculated.

3.4 NH_3-[SWNT-Sheet] system

The case interaction properties of ammonia (NH_3) with the Li[SWNT-Sheet] will now be discussed that is also shown in Fig. 3. In this structure we can see that in the localized sheet configuration the distance to the surface is around 2.67 Å with a HOMO/LUMO gap of 1.64 kcal/mol and an expulsion energy of 24.05 kcal/mol. Interestingly, in this case this species is the lowest energy structure as can be seen from the relative energies presented. The vibrational modes of $\nu_2 - \nu_3$ are larger than the isolated surfaces as we can see that is directly related to the insertion of the metal atom.

While the energy order has slightly shifted the barrier to move from the sheet to between the SWNT and the sheet is only 0.27 kcal/mol. The expulsion energy of these two configurations is quite similar as well. The distance between the SWNT and the sheet in this second configuration is 3.02 and 4.0 Å, respectively. The Li[SWNT-Sheet] stretching mode in this case is larger than the other cases that has a direct influence on the relative stability of this conformer. In the final encapsulated case, the energy of expulsion is 1.31 kcal/mol with an energy barrier of 22.74 kcal/mol that is almost three times higher than the non-metal case. In this species the interior vibrational mode (ν_5) being slightly elevated due to the interactions of the NH_3 with the walls of the SWNT cavity. For the NH_3 examples shown the adsorption energies are larger suggesting that the metal is indeed localized on the carbon surface.

4 Conclusions

In this study the ability of this so-called "scorpion" like Li[SWNT-Sheet] system in exploiting charge transfer effects to expunge molecules from the interior cavity of the SWNT. The metals lead to charge localization on surfaces to allow the polar molecules to be more stable on the exterior of the molecular species than on the interior of the nanotubes.

The barriers to move from the SWNT to the surface of the sheet of the polar molecule gradually increase as a result of charge transfer mechanisms. Interestingly, the barrier for the translation from the "between" configuration to the "sheet" configuration is minimal upon metal adsorption that denotes the greater affinity for alternatives to endohedral molecular encapsulation. The metals exert a force that is capable of extracting the molecules from the cavity of the SWNT.

The current method outlines a potential transport device strategy induced by the addition of external metal atoms. While in the previous study [21] we demonstrated the efficacy of the model in encapsulating molecules inside of the SWNT species this work proposes the contrary. Once the molecules are trapped a procedure for their expulsion must be devised. The reason as to why the polar molecules prefer the "between" configuration is related to the coupling of the valence electron donated by the metal atom and the polarizable species.

As we have shown [27] the distances between an excess electron and a polar molecule require spacing to eliminate unfavorable repulsion effects. However, without metals the polar molecules can smoothly progress from being on the surface of the sheet to the cavity of the SWNT. Upon encapsulation metals can be adsorbed readily (which is also evident from the favorable energies of adsorption in this work) that cause the sheet to attract the polar molecules thereby causing them to leave the interior of the SWNT molecule. This permits a molecular switch to form that can permit the encapsulation and expulsion of small polar species based on varying charge transfer capacities associated with metal adsorption.

We propose physical methods to improve the expulsion abilities of the polar species from the interior of the SWNT

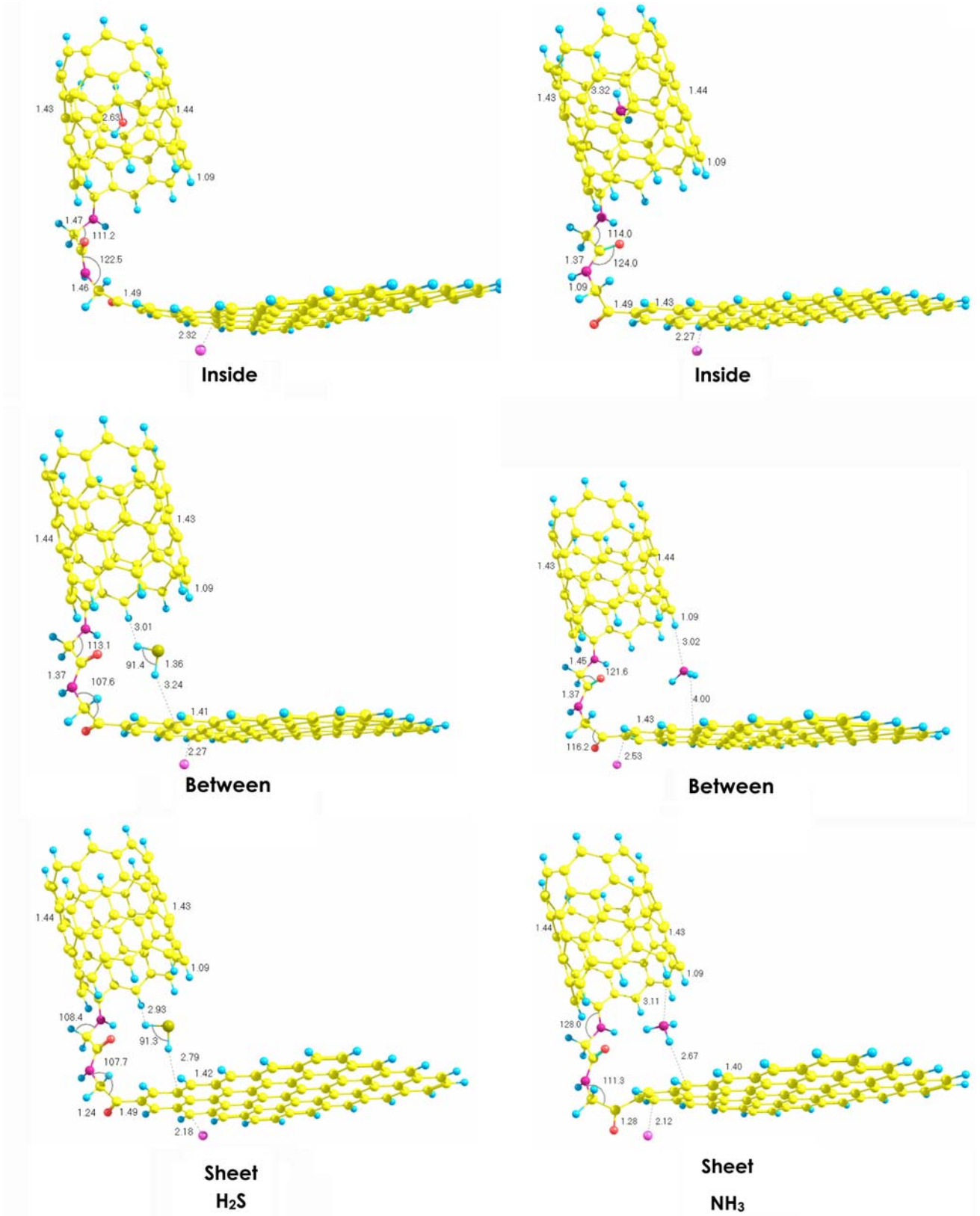

Fig. 3 Geometrical parameters of the H_2S and NH_3 systems whereby bond lengths are in angstroms (Å) and bond angles are in degrees (°). The same coloring scheme as in Fig. 2 is applied except for sulfur which is drawn in *green*

based on metal adsorption. The accurate characterization of these interactions demands further information on the electronic structure of the systems involved. These evaluations require insight into the electronic structure of the species involved. We propose that the results presented can be of use in the future synthesis of molecules used for drug delivery and catalysis.

Additionally, we have conducted some sample calculated on a simulated water environment. From the calculations there is a minor variation in the glycine geometry since it tends to assimilate differently. However, the general concepts and physical basis for the descriptors used remain consistent. It is our assertion that while biological substances are in solution the chemical adsorption we suggest in this model in vacuum can be directly applied since the effect of the metal atom is the key focal point being addressed herein.

An important issue that needs to be considered is the validity of the BLYP results that we have generated. There are several reports that account for their partially flawed nature and inability to describe dispersion. From recent studies we have demonstrated that such methods are useful to at least qualitatively yield information on fullerene and nanotube structures. Prof. Grimme [28–30] demonstrates that dispersion contributions contribute to the binding energies for some larger systems but the electrostatic differences can lead to physically reliable information. Their computations used modified GGA-DFT methods that yield superior energies even when compared to MP2 ab initioresults in various molecular systems. Preliminary tests in our group [31] have reported that the BLYP methods used have interesting correction terms which yield dissociation energies that are reliable in comparison to other functionals. In the comparison several competing methods and strategies were undertaken but the selected series shows the greatest empirical agreements.

It is understandable that dispersion problems can lead to difficulty in the analysis of the presented results. The calculations reported should serve as a qualitative guide in the understanding of novel devices for use as molecular traps. The BLYP theoretical DFT method is believed to be successful in the representation of the dispersion and intermolecular attractions. Comparisons to other DFT methods lead to generally well described results. There are few benchmarks available for systems of this study but on sample calculations of fullerenes and nanotubes the selected methodological framework appears to outperform available commonly implemented techniques. The BLYP platform has been normalized to larger nanoscale systems which makes its use optimal in these cases. In any case, the system is not yet experimentally viable and therefore the purpose of this current report is a qualitative model for a potential scheme of molecular expulsion from the interior cavities of nanotubes.

The "scorpion" shaped SWNT-Sheet can be coupled to metal atoms in order to temporarily trap organic molecules in the SWNT cavities. Upon the need to dispense such compounds metal atoms can be implemented to enhance this process. A reduced model has been used but it is our belief that the principles proposed should be consistent in larger scale systems.

Acknowledgments Financial and computational resources from the UNAM are deeply acknowledged.

References

1. Iijima S (1991) Nature 354:56. doi:10.1038/354056a0
2. Ge M, Sattler K (1994) Chem Phys Lett 220:192. doi:10.1016/0009-2614(94)00167-7
3. Guo Z, Sadler JPJ, Shik CT (1998) Adv Mater 10:701. doi:10.1002/(SICI)1521-4095(199806)10:9<701::AID-ADMA701>3.0.CO;2-4
4. Balavoine F, Schultz P, Richard G, Mallouh V, Ebbesen TW, Mioskowski C (1999) Angew Chem 38:1912. doi:10.1002/(SICI)1521-3773(19990712)38:13/14<1912::AID-ANIE1912>3.0.CO;2-2
5. Jarvis SP, Uchihashi T, Ishida T, Tokumoto H, Nakayama Y (2000) J Phys Chem B 104:6091. doi:10.1021/jp001616d
6. Trzaskowski B, Jalbout AF, Adamowicz L (2006) Chem Phys Lett 430:97. doi:10.1016/j.cplett.2006.08.125
7. Trzaskowski B, Jalbout AF, Adamowicz L (2007) Chem Phys Lett 446:314. doi:10.1016/j.cplett.2007.07.045
8. de Leon A (2008) Chem Phys Lett. doi:10.1016/j.cplett.2008.03.08
9. Contreras-Torres FF, Jalbout AF, Amelinas O, Basiuk VA (2008) J Phys Chem C 112:2736. doi:10.1021/jp710803j
10. Hu X, Li H, Ding J, Han S (2004) Biochemistry 43:6361. doi:10.1021/bi049859+
11. Sahai MA, Viskolcz B, Pai EF, Csizmadia IG (2007) J Phys Chem B 111:11592. doi:10.1021/jp073471h
12. Chen ECM, Chen ES (2007) E.S. Chem Phys Lett 435:331. doi:10.1016/j.cplett.2006.12.064
13. de Leon A, Jalbout AF, Basiuk VA (2008) Chem Phys Lett 452:306. doi:10.1016/j.cplett.2007.12.065
14. Zanella R, Basiuk EV, Santiago P, Basiuk VA, Mireles E, Puente-Lee I et al (2005) J Phys Chem B 109:16290. doi:10.1021/jp0521454
15. Chen Z, Yang Y, Chen F, Quan Q, Wu Z, Liu Z (2005) J Phys Chem B 109:11420. doi:10.1021/jp051848i
16. Durgun E, Dag S, Ciraci S (2004) Phys Rev B 70:155305. doi:10.1103/PhysRevB.70.155305
17. Arsenas JF, Lopez-Tocon I, Castro JL, Centeno SP, Lopez-Ramirez MR, Otero JC et al (2005) Spectr 36:515
18. Baber AE, Jensen SC, Hoshino M, Kaneko M (2003) J Phys Chem A 107:5523. doi:10.1021/jp034099i
19. Jalbout AF, del Castillo R, Adamowicz L (2007) Chem Phys Lett 445:89. doi:10.1016/j.cplett.2007.06.127
20. Liu L, Wang T, Li J, Guo Z-X, Dai L, Zhang D, et al (2003) Chem Phys Lett 367:747. doi:10.1016/S0009-2614(02)01789-X
21. de Leon A, Jalbout AF (2008) Chem Phys Lett. doi:10.1016/j.cplett.2008.04.030
22. Pavanello MA, Jalbout AF, Trzaskowski B, Adamowicz L (2007) Chem Phys Lett 442:339. doi:10.1016/j.cplett.2007.05.096
23. Jalbout AF, Organometall J (2008) Chem (Kyoto) 693:1143
24. Bakalis E, Zerbetto F (2007) ChemPhysChem 8:1005. doi:10.1002/cphc.200600715
25. Delley B (1990) J Chem Phys 92:508. doi:10.1063/1.458452

26. Jalbout AF (2008) J Theor Comput Chem 7:157. doi:10.1142/S0219633608003666
27. Jalbout AF, Adamowicz L (2007) Adv Quantum Chem 52:233
28. Mueck-Lichtenfeld C, Grimme S (2007) Mol Phys 105:2793. doi:10.1080/00268970701635543
29. Schwabe T, Grimme S (2007) Phys Chem Chem Phys 9:3387. doi:10.1039/b704725h
30. Neese F, Schwabe T, Grimme S (2007) J Chem Phys 126:124115/1
31. Jalbout AF (2008) J Phys Chem C (in press). doi:10.1021/jp800438r